Supporting Information

Bi-Axial Growth Mode of Au-TTF Nanowires Induced by Tilted Molecular Column Stacking

Yanlong Xing, [†,¶] *Eugen Speiser,* [†,*] *Dheeraj K. Singh,* [‡,§] *Petra S. Dittrich*[Δ] *and Norbert Esser*[†]

† Leibniz-Institut für Analytische Wissenschaften - ISAS- e. V, 12489 Berlin, Germany;

¶ School of Chemical and Environmental Engineering, Shandong University of Science and Technology, 266590 Qingdao, PR China;

‡ Department of Chemical Physics, Jacobs University, 28759 Bremen, Germany;

§ Department of Physics, Institute of Infrastructure Technology Research & Management, Ahmedabad, 380026, India;

Δ Department of Biosystems Science and Engineering, ETH Zurich, 4058 Basel, Switzerland.

Corresponding Author

* Eugen Speiser,

Tel: +49-231-1392-3552, Fax: +49-231-1392-3544,

E-mail: eugen.speiser@isas.de

Contents

S1. Images of a TTF Crystal and Au-TTF Nano-/Microwires

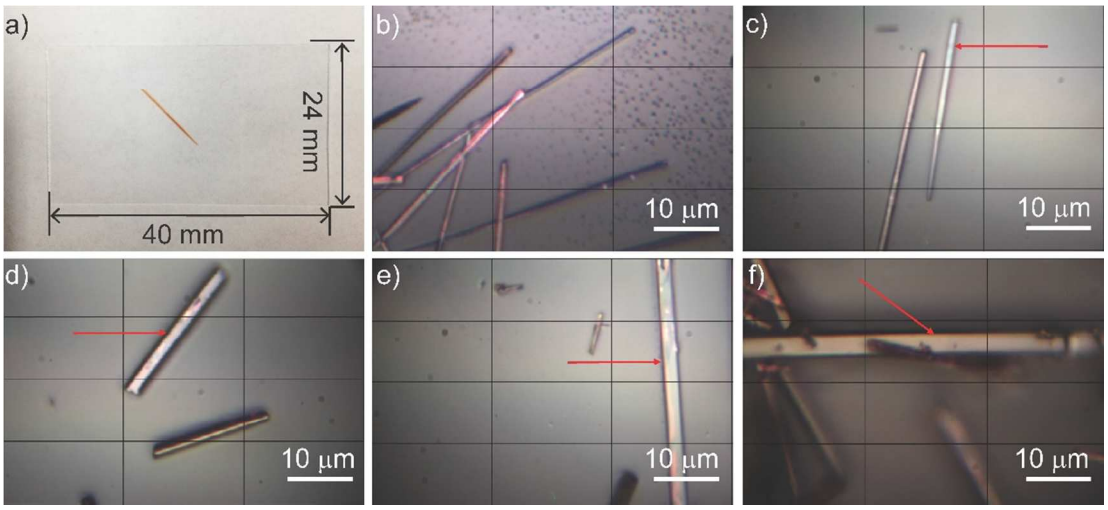

Figure S1. a) A picture of an orange TTF crystal (on a 24 × 40 mm glass slide). Images of Au-TTF wires under Raman microscope b) nanowires, diameter: 630 ± 130 nm; c) microwires, diameter ~ 1 μm; d) specified microwire, diameter ~ 2 μm; e) microwire, diameter ~ 3 μm; f) specified microwire, diameter ~ 4 μm. The red arrow specified the microwire for Raman measurement.

S2. Depolarization Ratio

The depolarization ratio (P) is defined as the ratio between the Raman signals obtained in the crossed polarization configuration (I_{xy}) and those obtained in the parallel configuration (I_{xx}):[1]

$$P = \frac{I_{xy}}{I_{xx}} \tag{S1}$$

It is a concept widely used to do quantitative analysis on the sample polarization response.[2] In this work, we analyzed the depolarization ratio based on the intensities of scattered laser light

from a single TTF crystal and Au-TTF nano-/microwires under crossed and parallel polarization configurations.

S3. Raman Tensors of Point Groups for TTF and TTF^+

Molecular vibrations can be described by the sum of vibrational normal eigen modes. It is possible to classify the normal vibrations by applying the group theory.[2] Each normal vibration will have a symmetry corresponding to one of the irreducible representations of the molecular point group. If a molecule has a center of inversion, the vibrations that are centrosymmetric show Raman active properties, which are usually labelled with the subscript *g*. The symmetry of a given vibrational mode is reflected in its corresponding Raman tensor.[1] Here, the Raman tensors for C_{2v} and D_{2h} point groups which are isomeric are shown in Table S1. The calculated A_{1g} Raman tensor elements for both TTF (C_{2v}) and TTF^+ (D_{2h}) are depicted in Table 1 (see manuscript).

Table S1. Raman tensors for the symmetry classes of the C_{2v} and D_{2h} point groups*

Point group	Symmetry class			
	A_{1g}	A_{2g}	B_{1g}	B_{2g}
C_{2v}	$\begin{pmatrix} a & 0 & 0 \\ 0 & b & 0 \\ 0 & 0 & c \end{pmatrix}$	$\begin{pmatrix} 0 & d & 0 \\ d & 0 & 0 \\ 0 & 0 & 0 \end{pmatrix}$	$\begin{pmatrix} 0 & 0 & e \\ 0 & 0 & 0 \\ e & 0 & 0 \end{pmatrix}$	$\begin{pmatrix} 0 & 0 & 0 \\ 0 & 0 & f \\ 0 & f & 0 \end{pmatrix}$
Point group	Symmetry class			
	A_{1g}	B_{1g}	B_{2g}	B_{3g}
D_{2h}	$\begin{pmatrix} a & 0 & 0 \\ 0 & b & 0 \\ 0 & 0 & c \end{pmatrix}$	$\begin{pmatrix} 0 & d & 0 \\ d & 0 & 0 \\ 0 & 0 & 0 \end{pmatrix}$	$\begin{pmatrix} 0 & 0 & e \\ 0 & 0 & 0 \\ e & 0 & 0 \end{pmatrix}$	$\begin{pmatrix} 0 & 0 & 0 \\ 0 & 0 & f \\ 0 & f & 0 \end{pmatrix}$

* Raman tensors of point groups are from Bilbao Crystallographic Server.

S4. X-ray Crystal Structure of Single TTF Crystals

TTF (referring to α-TTF, hereafter in the following text) shows a base-centered monoclinic lattice, with two molecules per unit cell as can be seen from X-ray diffraction data (Figure S1).[3-4] For neutral TTF molecules in a crystal, the atoms S1-S2-C3-C3B-S2B-S1B are in a common plane (Figure S2 and S3), as demonstrated in reported work.[5-6] The view from different planes indicates that there is an angle of 52.59^{o} between the two molecule planes (Figure S1).

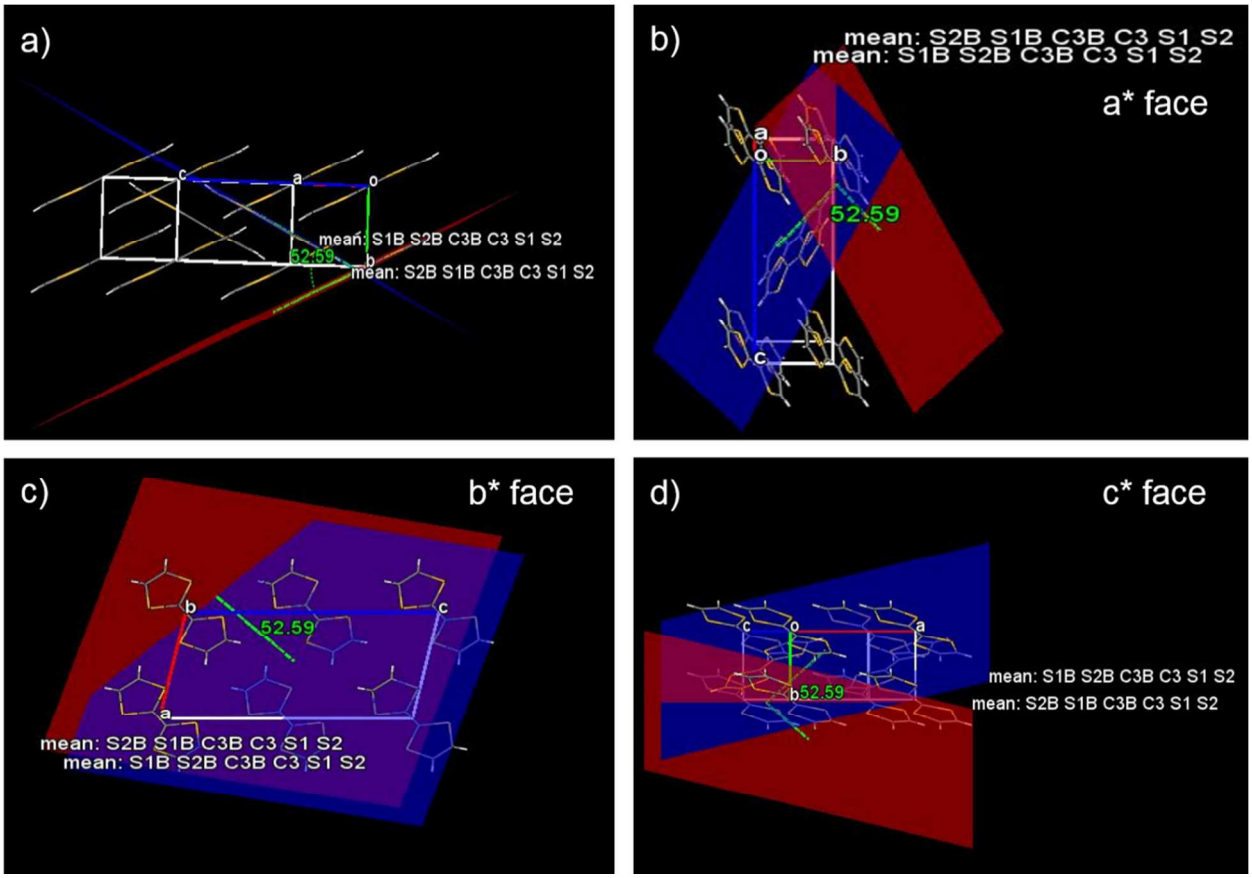

Figure S2. The view from different facets of crystalline TTF and the calculated angle between two TTF molecules in a unit cell of a TTF crystal (Cambridge Structural Database, reference code: BDTOLE10) in Mercury 3.6 software. a*, b*, c* faces refer to unit cell faces in single crystal, which are related to the crystal sketch in Figure S3a. Molecular planes were calculated from the central two C (C3, C3B) and four S (S1, S2, S2B, S1B) atoms of the TTF molecules

with different orientations. The angle between these two molecular planes (marked in red and blue planes separately) were calculated by the software to be 52.59°. The crystal structure was reported in previous work.[6]

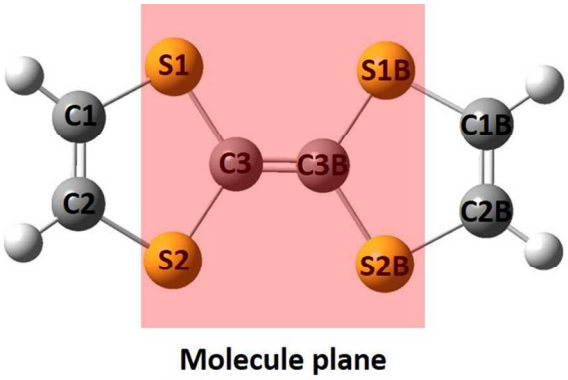

Figure S3. The labelling of atoms in the TTF molecule and the molecule plane as defined for angle measurement (marked in pink). TTF^{+} molecule is also labelled similarly.

S5. Angular Based Polarized Raman Spectra of a TTF Crystal

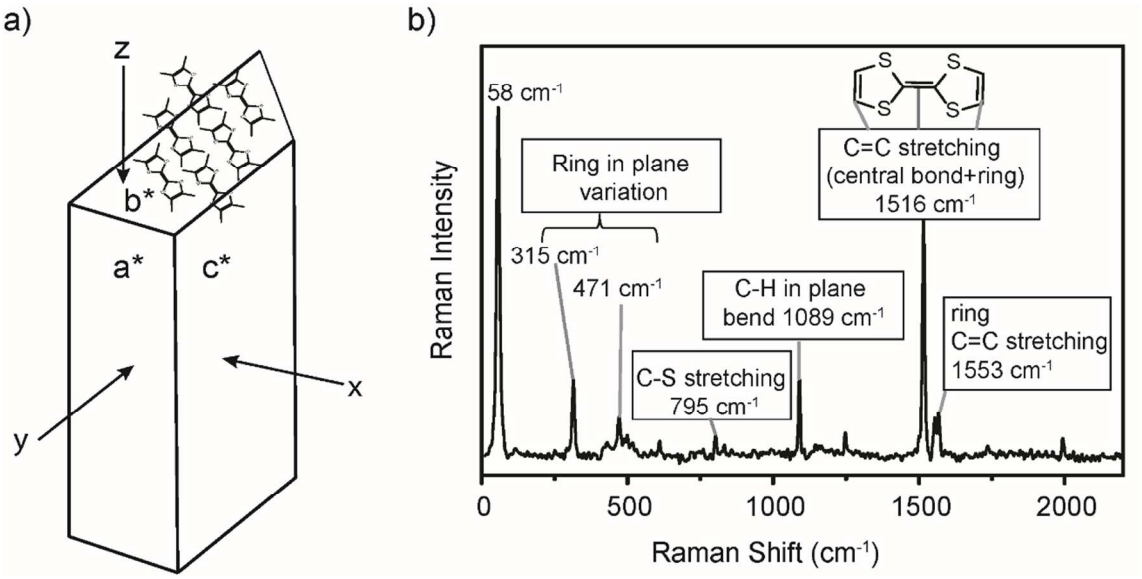

Figure S4. a) TTF crystal sketch with a*, b*, c* facets. x, y and z refer to the incident light directions. b) Full spectrum of a TTF crystal from the a* facet under parallel polarization

configuration, y(zz)$\bar{y}$.The peak at ~1516 cm^{-1} corresponds to central C=C bond (C3=C3B) and ring C=C bond (C1=C2 and C1B=C2B) stretching, and the peak at ~1553 cm^{-1} corresponds to ring C=C (C1-C2 and C1B=C2B) stretching. The numbering of C atoms refers to Figure S2. The peak at around 1250 cm^{-1} is assigned to a combined vibration (C-C-H bend + C-S stretching). It is very weak in the spectra of charged TTF (Figure 2), thus not discussed here.

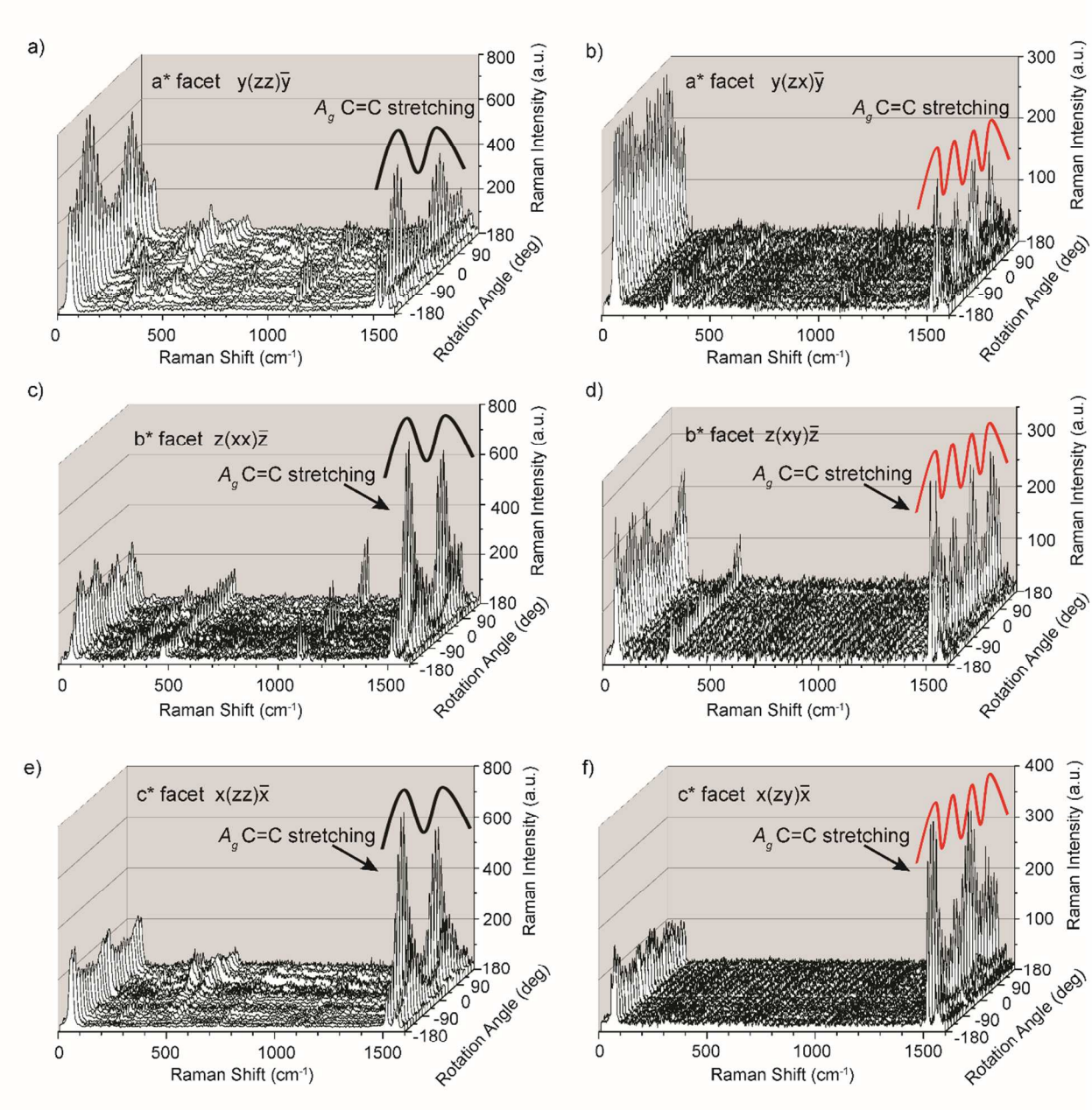

Figure S5. Angular variations of Raman spectra from different facets of a TTF crystal under the parallel and crossed polarization configurations. a) and b) are the rotational polarized Raman

spectra of the a* facet under parallel and crossed polarization, respectively. c) and d) are the spectra of the b* facet. e) and f) are the spectra of the c* facet. The molecular A_g vibrational mode (~1516 cm^{-1}, central bond and ring C=C stretching) vary in intensities by a periodicity of 180^o under parallel (black lines) and 90^o under crossed configurations (red lines). Typically, the peak at ~1516 cm^{-1} can be used for both qualitative and quantitative analysis. The a*, b*, c* facets of the crystal and xyz direction refer to Figure S3a, $\bar{x}$, $\bar{y}$, $\bar{z}$, indicate the direction of backscattered light. For rotation angle, 90^o was always defined at the highest intensity of 1516 cm^{-1} peak under parallel configuration.

Table S2 Results derived from the simulation of the depolarization ratio of a TTF crystal. α, β, γ are the Euler angles, *beta* is the angle between two TTF molecules and D is the constant factor.

Facet	α [°]	β [°]	γ [°]	D	*beta* [°]
a*	12.6	-76	138.2	0.081	51.4
b*	-161.8	-83.2	124.6	0.09	51.6
c*	25.4	-94.4	63.8	0.08	51.8
Average				0.08	51.6 ± 0.2

Besides the evaluation of the angle between the molecular planes in TTF crystal unit cell (as discussed in the manuscript), the orientation of the molecules with respect to the incoming laser beam direction was also determined. The molecular orientation of the TTF molecules in the crystal derived from sets of measurements on the three facets (a*, b* and c*) is in consistency with the orientations of the crystal structure for each scattering geometry.

S6. Equations of the Simulation of Depolarization Ratio

Equation S1and S2 illustrate the simulation of Raman intensity (I_{is}) under parallel (I_{xx}) and crossed (I_{xy}) configurations. In equation S1 for parallel configuration, the left vector $\begin{pmatrix}1\\0\\0\end{pmatrix}$ represents the polarization orientation of incoming light (e_i), while the right vector $\begin{pmatrix}1\\0\\0\end{pmatrix}$ representing the polarization orientation of scattered light (e_s). Similarly, in Equation S2 for crossed configuration, the left $\begin{pmatrix}1\\0\\0\end{pmatrix}$ represents the incoming light, while the right $\begin{pmatrix}0\\1\\0\end{pmatrix}$ represents the polarization orientation of scattered light. $M_{zxz}(\alpha,\beta,\gamma)$ represents the Euler rotation matrix. In equation S2 and S3, $\overline{\overline{R}}(\psi)$ is the Raman tensor while ψ is the angle of rotation around the X axis between the two molecular planes, as expressed in equation S4.

$$I_{xx} = \begin{pmatrix}1\\0\\0\end{pmatrix} \cdot M^{T}_{zxz}(\alpha,\beta,\gamma) \cdot \overline{\overline{R}}(\psi) \cdot M_{zxz}(\alpha,\beta,\gamma) \cdot \begin{pmatrix}1\\0\\0\end{pmatrix} \quad \text{(S2)}$$

$$I_{xy} = \begin{pmatrix}1\\0\\0\end{pmatrix} \cdot M^{T}_{zxz}(\alpha,\beta,\gamma) \cdot \overline{\overline{R}}(\psi) \cdot M_{zxz}(\alpha,\beta,\gamma) \cdot \begin{pmatrix}0\\1\\0\end{pmatrix} \quad \text{(S3)}$$

$$\overline{\overline{R}}(\psi) = M^{T}_{zxz}(0,\psi,0) \cdot \overline{\overline{R}}(0) \cdot M_{zxz}(0,\psi,0) \quad \text{(S4)}$$

S7. Raman Assignments of TTF^0, TTF^{n+} (0<n<1) and TTF^+

Table S3. Typical Raman mode assignments of TTF^0, TTF^{n+} (0<n<1) and TTF^+

Vibrational modes (A_g symmetry)*	TTF^0	TTF^{n+} (0<n<1)	TTF^+*
C=C stretching (ring)	1553 cm^{-1}	1513 cm^{-1}	1510 cm^{-1}
C=C stretching (central bond + ring)[1)]	1516 cm^{-1}		
C=C stretching (central bond)[2)]		1415 cm^{-1}	1516 cm^{-1}
C-H in plane	1089 cm^{-1}	1011 cm^{-1}	1088 cm^{-1}
C-S stretching	795 cm^{-1}	753 cm^{-1}	758 cm^{-1}
In-plane ring bend	471 cm^{-1}	504 cm^{-1}	506 cm^{-1}

* The symmetry species numbers, frequencies of TTF^+ see Reference.[7] Raman shifts for TTF^0 and TTF^{n+} (0<n<1) are the results from this work. The B_g mode peak at 58 cm^{-1} is not studied in this work and thus not included in the table. The A_g mode peak at 315 cm^{-1} and 1250 cm^{-1} for TTF crystal is not observed or very weak in the spectra of TTF^{n+} (0<n<1) and TTF^+. The A_g mode peak at 1369 cm^{-1} for TTF^{n+} (0<n<1) is very weak in in the spectra of TTF crystal. Thus, these peaks are not discussed here, as well as the peaks at wavenumber above 1600 cm^{-1}.

1) The C=C stretching (central bond + ring) mode was used for angular based polarized Raman analysis on TTF crystal.

2) The C=C stretching (central bond) mode was used for angular based polarized Raman analysis on Au-TTF nanowire.

S8. Angular Based Polarized Raman Spectra of Au-TTF Nanowires

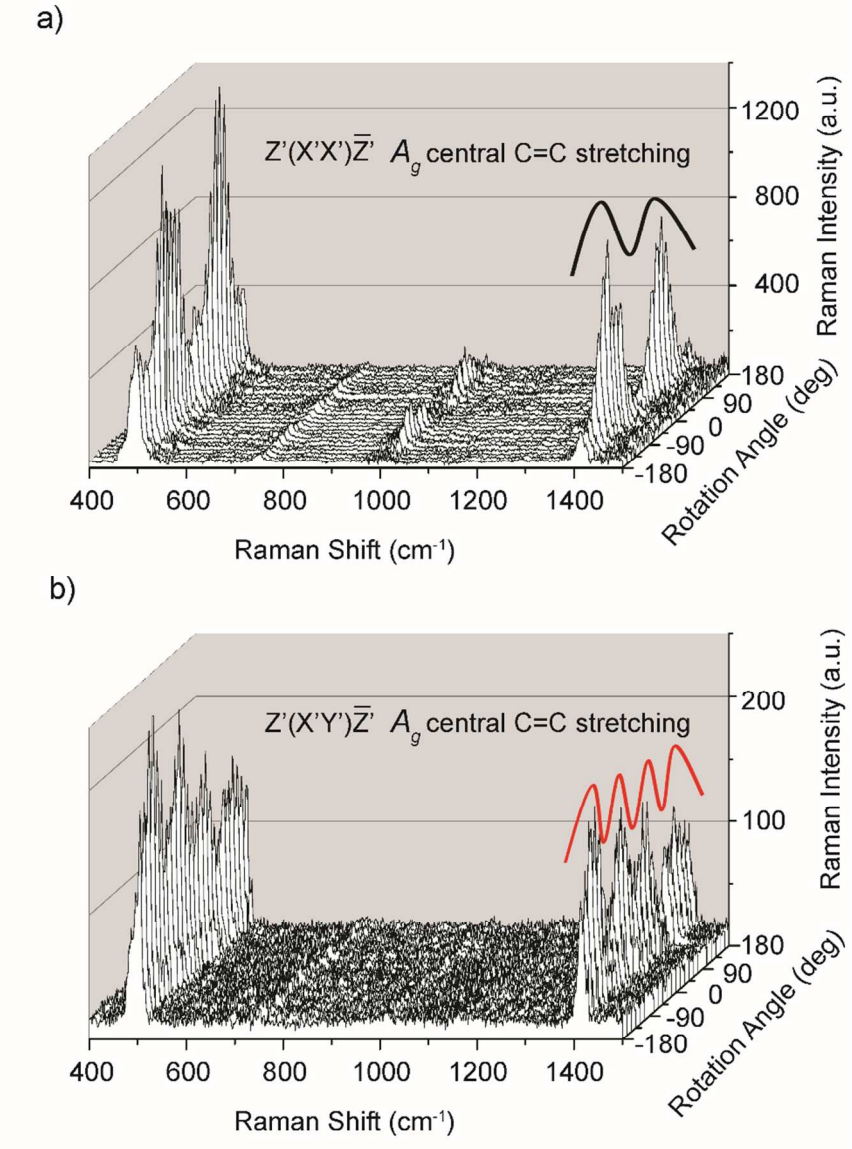

Figure S6. Angular variation of Raman spectra of a single Au-TTF nanowire under parallel and crossed polarization configurations. The molecular A_g vibrational mode (central C=C bond stretching, at ~1415 cm^{-1}) varies in intensity by a periodicity of 180° under parallel (figure a, black line) and 90° under crossed configurations (figure b, red line). The X′Y′Z′ configurations refer to Figure 2 inset, $\bar{Z}'$ indicates the direction of backscattered light of Z′. For rotation, angle 90° was always defined at the highest intensity of 1415 cm^{-1} peak under parallel configuration.

S9. Raman Intensity Curves of Peaks at 1415 cm^{-1} for Different Nano-/Microwires

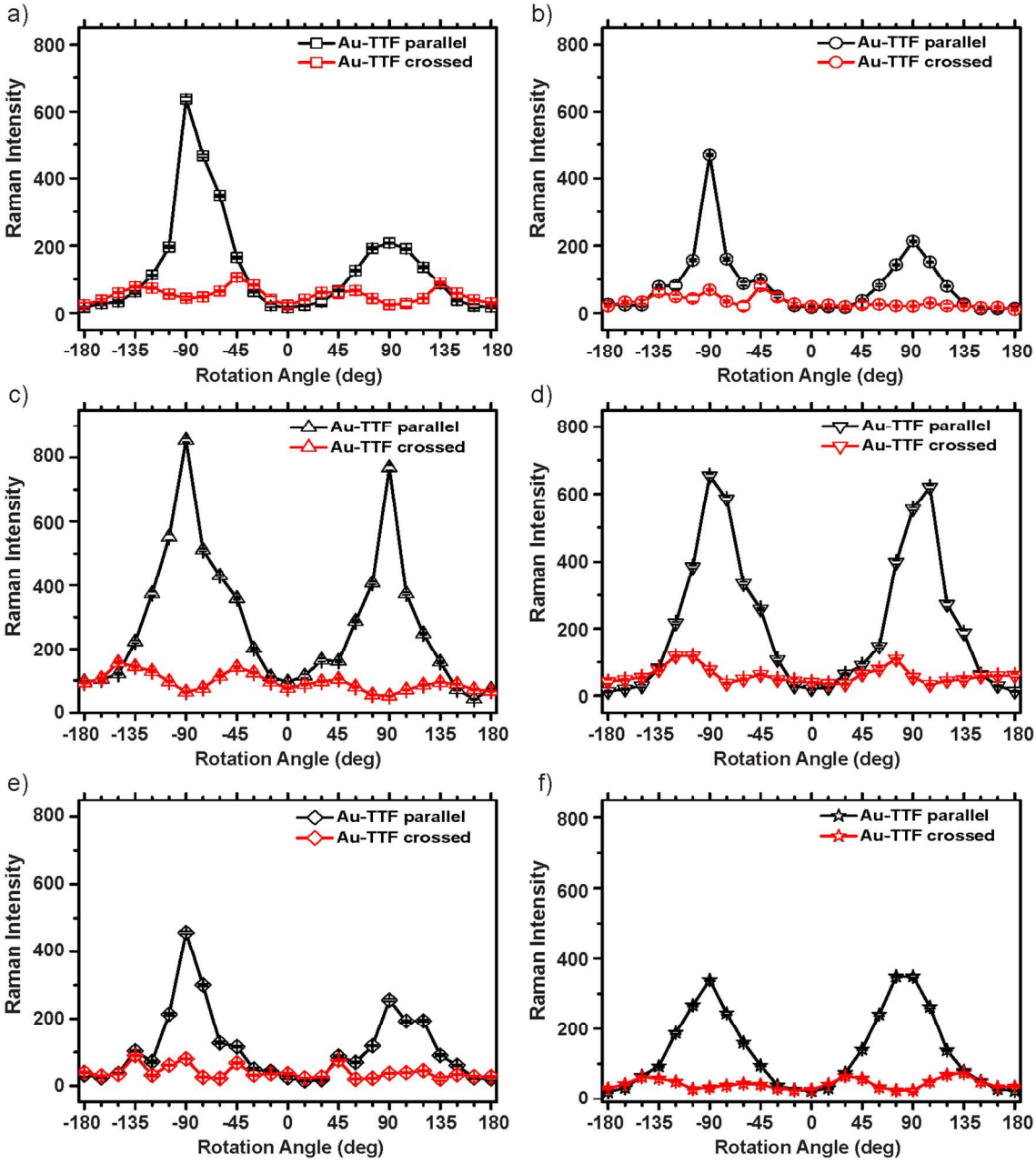

Figure S7. Angular dependence of Raman intensity (A_g mode at 1415 cm^{-1}) for six different nanowires under parallel (I_{xx}, black hollow symbols) and crossed (I_{xy}, red hollow symbols) configurations.

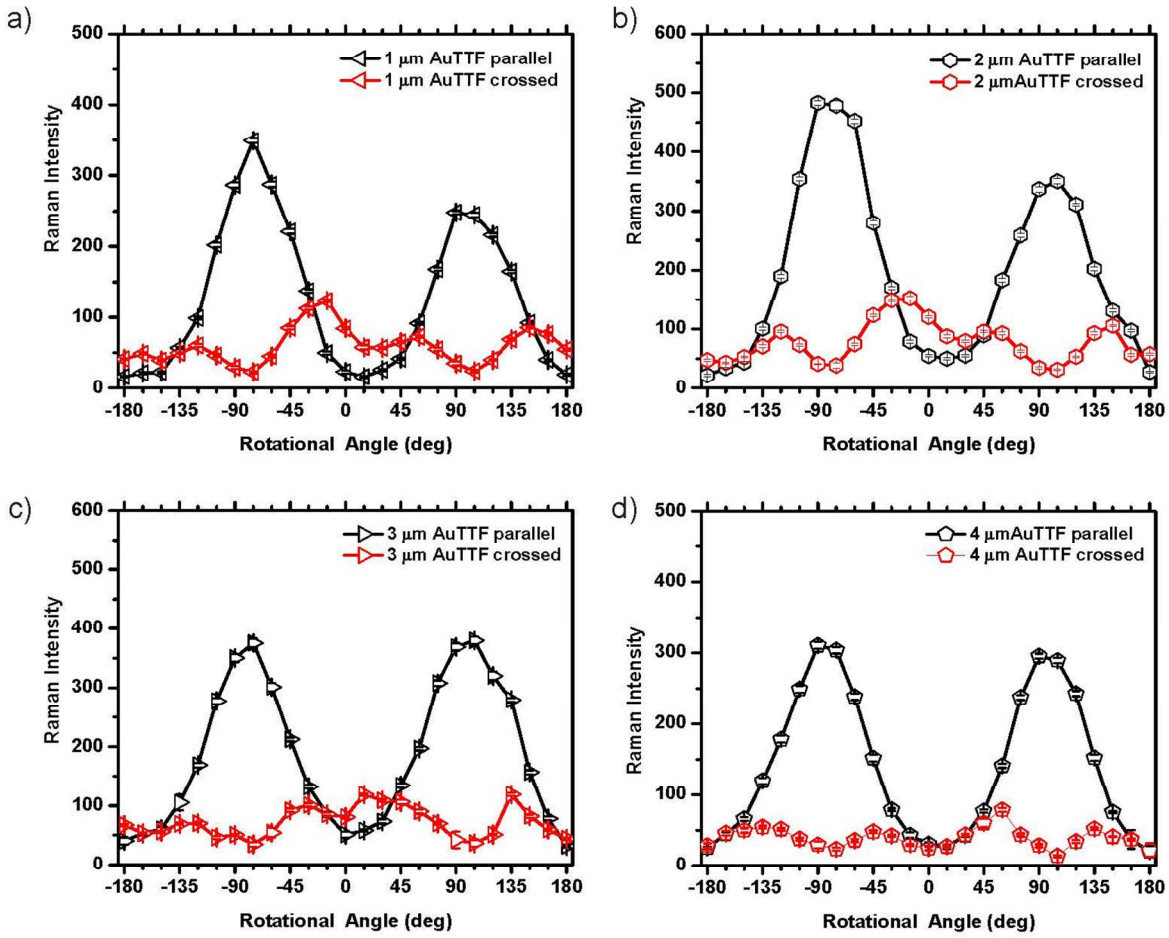

Figure S8. Angular dependence of Raman intensity (A_g mode at 1415 cm^{-1}) for four different microwires under parallel (I_{xx}, black hollow symbols) and crossed (I_{xy}, red hollow symbols) configurations.

S10. Simulation of Depolarization Ratio of Au-TTF Microwires

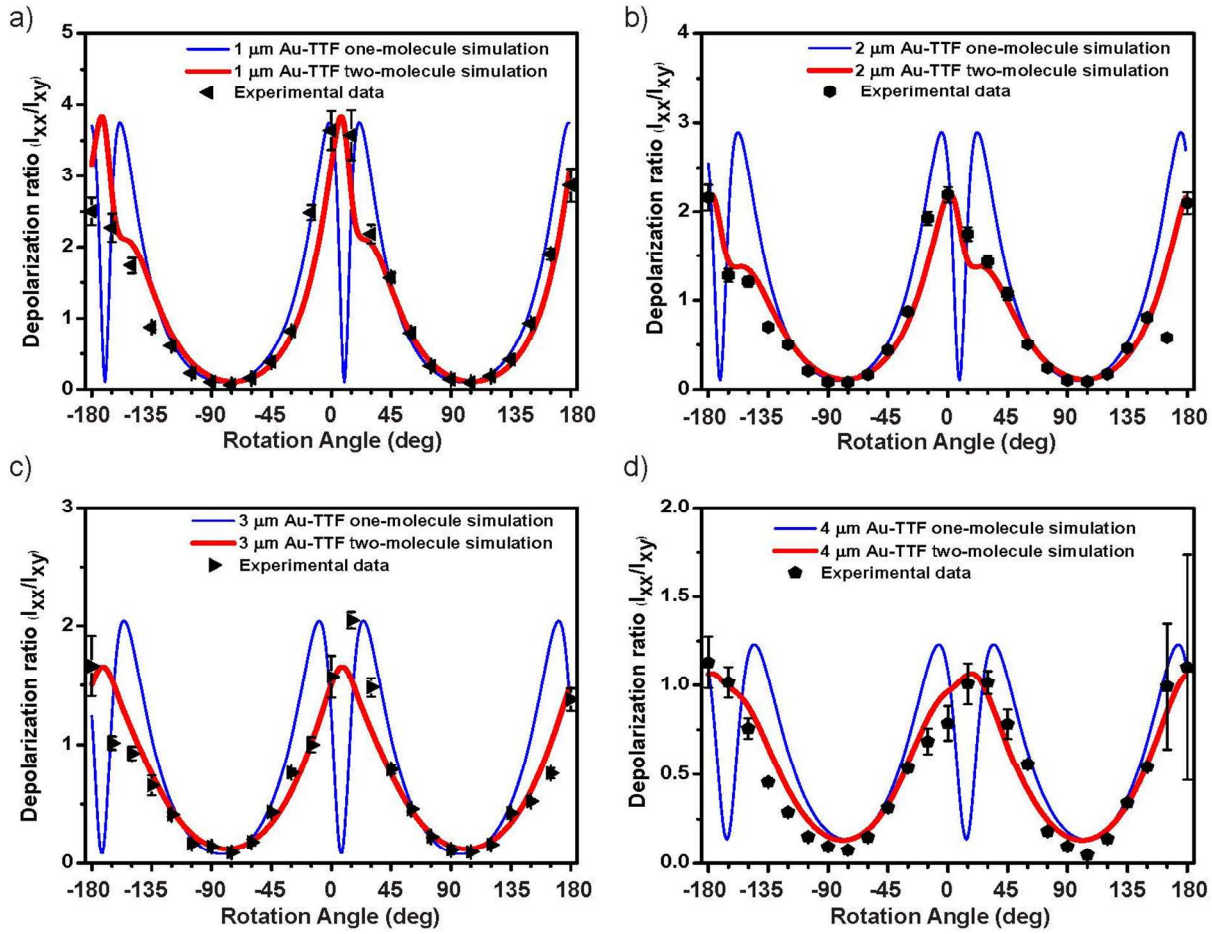

Figure S9. Depolarization ratio of four different Au-TTF microwires. Experimental (symbols) and simulated (lines) depolarization ratio of the Raman intensity of the ~1415 cm^{-1} (central C=C bond stretching) vibration. The experimental data were calculated from the angular dependent Raman intensity shown in Figure S8. The blue lines are the one-molecule simulations, while the red lines are the two-molecule simulations. The Pearson correlation coefficients between fitted two-molecule lines (red) and experimental data are 0.904 (a), 0.901 (b), 0.878 (c) and 0.920 (d).

The simulated results of the different Au-TTF microwires are shown in Table S4 (SI), including the Euler angles (α, β, γ), polarization error D, angle between two molecule planes (ψ) and the angle (A_w) between molecule A (Y axis) and the longitudinal axis X' of the wire.

Table S4 Results derived from the two-molecule simulation of the depolarization ratio of different Au-TTF microwires (Figure S8).

No.	Diameter[μm]	α [°]	β [°]	γ [°]	D	ψ [°]	A_w [°]
a)	1	38.4	153.2	130.4	0.083	52	20.14
b)	2	43	154.2	132.4	0.081	51.6	20.19
c)	3	42	156	132.8	0.074	53.2	20.03
d)	4	49.2	155.4	140.6	0.084	56.6	20.36
	Average angle					53.4 ± 4.5	20.2 ± 0.3

S11. 3D Structure Model of an Au-TTF Nanowires

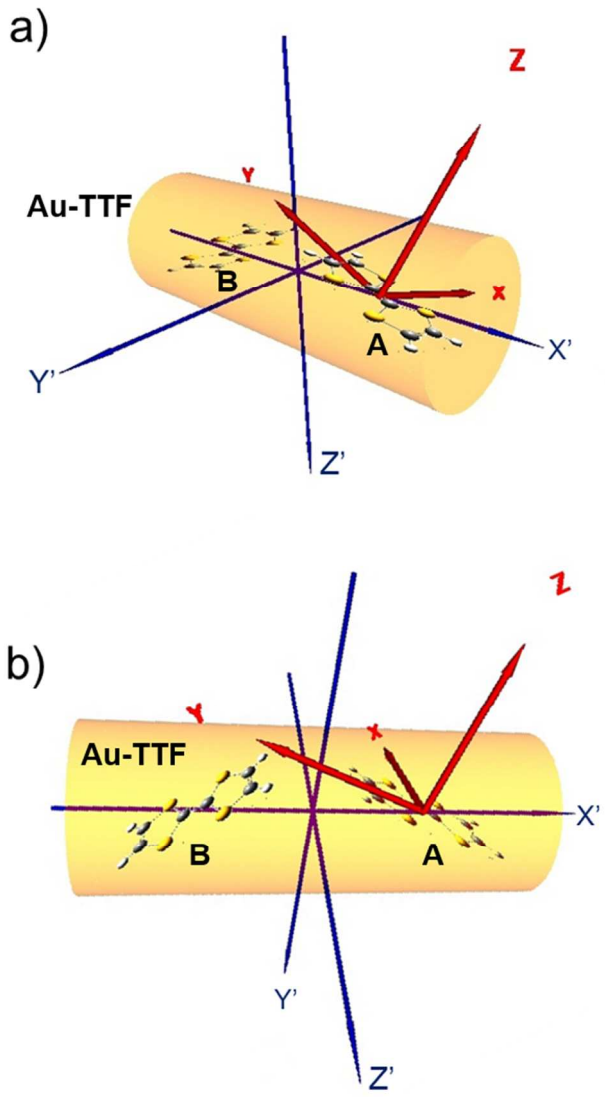

Figure S10. 3D model of an Au-TTF wire showing the rotation of molecules: a) view from side; b) view from front. The yellow cylinder indicates an Au-TTF nanowire with the two molecules inside the wire unit cell. Blue X'Y'Z' coordinates refer to the wire coordinates (the same as that shown in Figure 2 inset), where the blue X' is the longitudinal axis of wire. The red XYZ are the coordinates of molecule A, which are in accordance with the ones used in the DFT calculations (Table 1 in manuscript). Molecule A and molecule B represent the two different molecular orientations inside a single Au-TTF wire. The partially charged TTF^{n+} ($0<n<1$) molecule A is firstly positioned according to the Euler's angle (α, β, γ) (Table 2), then molecule B is tilted with the angle ψ around X axis of molecule A.

REFERENCES

(1) Zahn, D. R. T.; Gavrila, G. N.; Salvan, G. Electronic and Vibrational Spectroscopies Applied to Organic/Inorganic Interfaces. *Chem. Rev.* **2007**, *107*, 1161–1232.

(2) Singh, D.; Vikram, K.; Singh, D. K.; Kiefer, W.; Singh, R. K. Raman and DFT Study of Hydrogen-bonded 2- and 3-Chloropyridine with Methanol. *J. Raman Spectrosc.* **2008**, *39*, 1423–1432.

(3) Wudl, F.; Kaplan, M. L.; Hufnagel, E. J.; Southwick, E. W. Convenient Synthesis of 1,4,5,8-Tetrahydro-1,4,5,8-tetrathiafulvalene. *J. Org. Chem.* **1974**, *39*, 3608–3609.

(4) Sandman, D. J.; Epstein, A. J.; Chickos, J. S.; Ketchum, J.; Fu, J. S.; Scheraga, H. A. Crystal Lattice and Polarization Energy of Tetrathiafulvalene. *J. Chem. Phys.* **1979**, *70*, 305–313.

(5) Cooper, W. F.; Kenny, N. C.; Edmonds, J. W.; Nagel, A.; Wudl, F.; Coppens, P. Crystal and Molecular Structure of the Aromatic Sulphur Compound 2,2'-Bi-1,3-dithiole. Evidence for D-Orbital Participation in Bonding. *J. Chem. Soc. Chem. Commun.* **1971**, 889–890.

(6) Wang, X.; Broch, K.; Scholz, R.; Schreiber, F.; Meixner, A. J.; Zhang, D. Topography-Correlated Confocal Raman Microscopy with Cylindrical Vector Beams for Probing Nanoscale Structural Order. *J. Phys. Chem. Lett.* **2014**, *5*, 1048–1054.

(7) Siedle, A. R.; Candela, G. A.; Finnegan, T. F.; Vanduyne, R. P.; Cape, T.; Kokoszka, G. F.; Woyciejes, P. M.; Hashmall, J. A. Copper and Gold Metallotetrathiaethylenes. *Inorg. Chem.* **1981**, *20*, 2635–2640.